The Androgen Receptor T877A Mutant Recruits LXXLL and FXXLF Peptides Differently than Wild-Type Androgen Receptor in a Time-Resolved Fluorescence Resonance Energy Transfer Assay

Mary Szatkowski Ozers,[⊥] Bryan D. Marks,* Krishne Gowda, Kevin R. Kupcho, Kerry M. Ervin,[‡] Therese De Rosier, Naveeda Qadir,[#] Hildegard C. Eliason, Steven M. Riddle, and Mohammed Saleh Shekhani[§]

Invitrogen Discovery Sciences, 501 Charmany Drive, Madison, Wisconsin 53719

Received June 30, 2006; Revised Manuscript Received October 17, 2006

ABSTRACT: The interactions of the ligand binding domain (LBD) of androgen receptor (AR) and the AR T877A mutant, found in prostate cancer, with peptides from coactivator and corepressor proteins or random phage display peptides were investigated using in vitro time-resolved fluorescence resonance energy transfer (TR-FRET). Interaction of wild-type AR LBD with the random phage display peptide D11FxxLF was observed with dihydrotestosterone (DHT), testosterone, R1881, estradiol, spironolactone, progesterone, and cortisol resulting in distinct dose dependency (EC_{50}) values for each ligand and correlating well with the reported rank order potency of these agonists. Increasing concentrations of cyproterone acetate and mifepristone resulted in more complete disruption of the DHT-mediated AR-D11FxxLF peptide interaction, while flutamide, hydroxyflutamide, and bicalutamide caused only partial disruption of the complex. The mutant AR T877A LBD exhibited increased binding affinities for all ligands tested except for bicalutamide, mifepristone, DHT, and R1881 in a competitive binding assay as compared to wild-type AR LBD. This mutation was also characterized by increased ligand potency for agonist-induced peptide recruitment. Although usually an antagonist, hydroxyflutamide was more potent in the recruitment of D11FxxLF or an SRC3−1 LXXLL motif to AR T877A LBD than AR LBD. The antagonist cyproterone acetate behaved as a full antagonist of D11FxxLF recruitment to AR LBD and AR T877A LBD but as a more potent agonist in the recruitment of SRC3−1 to AR T877A LBD. These results suggest that the AR T877A mutation affects both ligand affinity and ligand dose dependency for peptide recruitment and may explain in part the altered responses of antagonists and increased transcriptional activation reported in androgen-independent prostate cancers.

Androgen receptor (AR)[1] is a transcription factor that is involved in the ligand-inducible gene regulation of male sexual development, prostate growth, spermatogenesis, and bone metabolism. The physiological ligands for AR are the steroid testosterone and the testosterone metabolite, dihydrotestosterone (DHT). Upon binding hormone, AR undergoes a conformational change that causes chaperone proteins to dissociate and results in translocation of AR from the cytoplasm to the nucleus, binding to DNA at androgen response elements located in the promoter region of androgen-responsive genes, and the subsequent association with coactivator proteins (*1*, *2*). Similar to the other steroid hormone receptors, AR consists of an N-terminal transactivation function (AF1), a DNA-binding domain, and a C-terminal ligand binding domain (LBD) that contains a second transactivation region (AF2). The LBD also contains the major recognition sites for coactivator interaction, via the LXXLL or FXXLF nuclear receptor interaction motifs found in most coactivator proteins including AR-specific coactivators ARA70, ARA54, and ARA55 (*3*−*7*). Unlike most other nuclear receptors, AR undergoes an agonist-induced intradomain interaction between an FXXLF motif in the N-terminal AF1 and the LBD, which has been shown to be important for transcriptional activation (*8*−*10*). Coactivator proteins are recruited to the agonist-occupied conformation of AR bound at promoters and possess histone acetyltransferase activity that results in unwinding of local chromatin structure for access by pol II and other transcription machinery.

Recent studies have indicated that AR is expressed in most prostate tumors of all stages, and mutated forms of AR are present in late-stage metastatic tumors (*11*−*14*). While the

* To whom correspondence should be addressed. Phone: 608-204-5102. Fax: 608-204-5300. E-mail: bryan.marks@invitrogen.com.

[⊥] Current address: University of Wisconsin-Madison, Department of Biochemistry, 433 Babcock Drive, Madison, Wisconsin 53706.

[‡] Current address: Quintessence Biosciences, Inc., 505 South Rosa Road, Madison, Wisconsin 53719.

[#] Current address: University of Wisconsin-Madison, Madison, Wisconsin 53706.

[§] Current address: Madison Molecular Research, LLC, 2901 Brian Lane, Madison, Wisconsin 53711.

[1] Abbreviations: AR, androgen receptor; LBD, ligand binding domain; TR-FRET, time-resolved fluorescence resonance energy transfer; DHT, dihydrotestosterone; AF, activation function; PSA, prostate specific antigen; GST, glutathione *S*-transferase; WT, wild-type; DMSO, dimethylsulfoxide; OHF, hydroxyflutamide; CPA, cyproterone acetate; Tb, terbium; CoRNR, corepressor nuclear receptor box; SRC, steroid receptor coactivator; Mif, mifepristone; Bic, bicalutamide; Flut, flutamide; Prog, progesterone.

10.1021/bi061321b CCC: $37.00
Published on Web 12/22/2006

detection of prostate abnormalities has greatly improved with prostate-specific antigen (PSA) tests, prostate cancer remains the second leading cause of cancer death in men (*15*). Treatment of prostate cancer by androgen ablation therapy via surgery or luteinizing hormone-releasing hormone agonists combined with androgen blockade therapy using anti-androgens often works for a limited time before the tumor becomes resistant (*14*, *16*). This resistance has been attributed to AR gene amplification (*17*−*19*), mutation of the AR leading to altered ligand specificity (*20*−*22*), and altered expression of coactivators (*23*−*25*). A number of mutation hotspots are found in the LBD, including the prevalent point mutation found in prostate cancer in which threonine 877 is replaced with alanine (T877A) (*11*, *14*, *26*, *27*). Crystallography indicates that this residue contacts the 17β-hydroxyl group of androgens (*28*−*31*). The T877A mutation has been shown to expand the ligand binding capacity of AR for different ligands and cause abnormal induction of gene expression (*22*, *26*). AR containing this T877A mutation is characterized by structural alterations in the binding pocket facilitating interaction with ligands such as progesterone, estradiol, and anti-androgens, which bind to the wild-type receptor with reduced affinity (*26*, *29*, *30*, *32*, *33*). The T877A mutation, found in the prostatic carcinoma cell line LNCaP, also appears to be responsible for differential ligand effects, causing some antagonists such as hydroxyflutamide (OHF) and cyproterone acetate (CPA) to behave as agonists (*34*, *35*). In addition to its role in reproductive cancers, AR has been found in osteoclast cells where it is believed to play a role in bone deposition and prevention of osteoporosis in men (*36*).

Wild-type AR has been shown to interact strongly with the AR N-terminal ^{23}FQNLF^{27} motif and to favor interaction with FXXLF motifs from ARA70 and ARA54 over the LXXLL motifs of the SRC/p160 coactivator family (*37*−*40*), although some higher affinity interactions with SRC LXXLL motifs have been reported (*7*). Charged sequences in the AR LBD AF2 domain, especially E709, E893, K720, K717, R726, and to a lesser extent E897, are known to modulate coactivator recruitment, and sequences flanking the FXXLF motifs help determine binding specificity to the LBD (*37*−*39*). Until recently, comparison of coactivator interactions with the T877A mutant AR has been lacking. Mifepristone, an antagonist of progesterone receptor and glucocorticoid receptor, was reported to inhibit R1881-induced coactivator interaction with AR and the T877A mutant and also mediated corepressor binding to AR (*41*). In very recent studies, the T877A mutant was characterized by a slower ligand dissociation rate for androgens R1881, DHT, and testosterone but did not exhibit an increased binding for FXXLF or LXXLF motifs in the presence of androgens (*42*).

Since all prostate cancers eventually become refractory to anti-androgen therapy, new pharmaceutical approaches may involve targeting the protein−protein interactions of coregulators with AR. Toward the goal of comparing ligand affinity differences and peptide recruitment for the wild-type AR and T877A mutant, we have examined the effects of agonists and antagonists on ligand-induced recruitment of a panel of peptides derived from known coactivators and corepressors as well as random phage display peptides. The experiments herein measure the ligand affinity using a competitive binding assay and quantify the dose dependency of peptide interactions with AR versus the AR T877A mutant using TR-FRET. Our results indicate that both the ligand affinity for the receptor and the ligand dose dependency for AR interactions with the peptides D11FxxLF and SRC3−1 differ between the wild-type AR LBD and the LBD bearing the T877A mutation.

MATERIALS AND METHODS

Materials. The peptides were synthesized and labeled with fluorescein (Fl) at the N-terminus by Anaspec (San Jose, CA) or were purchased from Anaspec with a reactive cysteine at the N-terminus, labeled using fluorescein-maleimide (Invitrogen/Molecular Probes; Eugene, OR), and purified by HPLC. The peptides were quantified by measuring the absorbance at 493 nm in 0.1 N NaOH, and the concentration was calculated using the extinction coefficient of 73 000 cm^{-1} M^{-1} for fluorescein.

Black assay plates were 384-well low-volume plates from Corning (Cat. No. 3676; Corning, NY) for a 20 μL assay volume. Ligands were diluted in 96-well polypropylene plates from Nalge Nunc (Rochester, NY) or 384-well polypropylene plates from Costar/Corning (Corning, NY). The ligand 2-hydroxyflutamide (OHF) was purchased from LKT Labs (St. Paul, MN). Bicalutamide was from Toronto Research Chemicals (Ontario, Canada). R1881 was purchased from Perkin-Elmer (Wellesley, MA). All other ligands were from Sigma Chemical Co. (St. Louis, MO). The terbium (Tb) anti-GST antibody, Fluormone AL Red, and assay buffers were from Invitrogen (Madison, WI). AR Red screening buffer (part no. PV4295) was used for the competitive ligand binding assay, and AR Green assay buffer (part no. P3011) was used for the peptide-based TR-FRET assay. Both buffers were completed by addition of DTT to a final concentration of 5 mM immediately prior to use.

Expression and Purification of AR Ligand Binding Domains. The rat wild-type AR sequences corresponding to the protein domain bearing the hinge and ligand binding domains (amino acids 606−902; NP_036634) and tagged with both glutathione S-transferase (GST) and 6x Histidine (His) at the N-terminus were sub-cloned into a pFastBac I vector (Invitrogen Corp., Carlsbad, CA). This vector was used to create a bacmid for recombinant baculovirus production in the Bac-to-Bac system (Invitrogen Corp., Carlsbad, CA). The 64 MW protein was found in the inclusion bodies of the recombinant-baculovirus infected BTI-TN-5B1-4 Trichoplusia ni cells (HighFive, Invitrogen Corp., Carlsbad, CA) and purified by denaturation, renaturation, and concentration by ammonium sulfate precipitation to a physical purity of at least 85%. The rat AR LBD is identical in sequence to the human AR LBD and is referred to as wild-type AR (WT AR). A mutated version of the rat AR LBD bearing a threonine to alanine change corresponding to residue 877 (AR T877A) in the human numbering was prepared using the Quick-Change Site Directed Mutagenesis kit from Stratagene (LaJolla, CA) and expressed and purified as described above. The active concentration of receptor was assessed by quantitation of [^{3}H]-methyltrienolone:receptor complexes using a hydroxylapatite (HAP) assay. The percent total of active AR, based on the [^{3}H]-methyltrienolone HAP assay, was typically between 5 and 10% (lowest estimate).

Competitive Binding TR-FRET Assay. The relative binding affinities of a panel of ligands for both WT AR and AR

T877A were measured by the ability of these compounds to displace a fluorescently labeled AR ligand, Fluormone AL Red, from AR. IC_{50} determinations for the panel of ligands were performed by testing each ligand at concentrations typically ranging from 30 μM to 2 pM (some lower-affinity ligands were tested using higher concentrations) using 3-fold serial dilution steps (each data point in duplicate) to generate a 16-point dose−response curve. Serial dilutions of each ligand were first prepared at 100× concentration in DMSO and then diluted to 4× concentration (at 4% DMSO) in assay buffer. Additions to the assay wells were made in the following order: ligand dilutions or DMSO solvent control; 1 nM AR LBD; 10 nM Fluormone AL Red/5 nM Tb anti-GST antibody. Maximum displacement of Fluormone AL Red was measured in control wells containing 10 μM DHT on each plate. Plates were incubated for 6 h at room temperature (22 °C). TR-FRET was then measured as described in Measurement of TR-FRET (below) except a different set of emission filters were used: the second terbium emission peak was detected using a 546-nm filter (10-nm bandwidth) and the emission of receptor-bound Fluormone AL Red was detected using a 570-nm filter (10-nm bandwidth).

Determination of LXXLL and FXXLF Peptide Interaction. Peptides that interacted with AR LBD were screened in assay wells containing a mixture of 20 nM AR LBD plus 5 μM ligand or an equivalent amount of DMSO, 1 μM Fl-labeled peptides, and 5 nM Tb anti-GST antibody added in AR Green assay buffer to a 384-well plate in a final volume of 20 μL. The plate was mixed gently, covered to protect from light, and stored at room temperature for 4 h. The TR-FRET ratio was measured as described below.

Peptide Titration. Fl-labeled peptide was serially diluted into AR Green assay buffer in a 384-well assay plate with final reaction conditions containing 20 nM AR LBD GST and 5 μM ligand (or equivalent volume of DMSO), followed by addition of Tb anti-GST antibody to a final concentration of 5 nM. Assay plates were either the 384-well black cliniplate (LabSystems; Franklin, MA) for a 40 μL volume or the low volume 384-well plate for a 20 μL volume (Corning; Corning, NY). The plate was mixed gently and incubated at room temperature protected from light. The TR-FRET ratio was measured after a 4 h incubation.

Peptide affinity for the DHT-occupied receptor was estimated in assays that contained increasing concentration of Fl-peptide plus 5 nM AR LBD GST or AR T877A LBD GST, 5 μM DHT, and 5 nM Tb anti-GST antibody. A parallel titration was conducted in the absence of receptor. To correct for diffusion-enhanced FRET, the sensitized emission from fluorescein (520 nm) in the absence of receptor was subtracted from the sensitized emission from fluorescein (520 nm) in the presence of DHT-occupied receptor and plotted against peptide concentration to determine approximate affinity values.

Agonist Ligand Titrations. Test ligands were diluted to 100× concentration in DMSO, and serial dilutions in DMSO were performed to maintain ligand solubility in a multi-well polypropylene plate. The test ligands were then diluted to 2× final concentration in AR Green assay buffer in the polypropylene plate, followed by transfer of 10 μL of each dilution to a 384-well black assay plate. Each well in the 384-well assay plate then received 5 μL of a 4× AR LBD GST dilution prepared in AR Green assay buffer and 5 μL of a 4× pre-mixture of Fl-labeled D11FxxLF peptide and Tb anti-GST anti-body. Final assay conditions after all additions were 5 nM receptor, 500 nM Fl-labeled D11FxxLF, 5 nM Tb anti-GST antibody, and 1% DMSO. DMSO was included as a constant concentration because it is a common solvent in compound libraries. Appropriate controls included replicate wells that contained no agonist (control for ligand-independent binding), no AR LBD GST protein (negative control for diffusion-enhanced FRET), and maximum agonist (positive control). The plate was gently agitated, incubated at room temperature, and protected from light prior to TR-FRET measurement.

Antagonist Ligand Titrations. As above, test antagonists were diluted to 100× concentration in DMSO, and serial dilutions in DMSO were performed to maintain ligand solubility in a multi-well polypropylene plate. The test antagonists were then diluted to 2× final concentration in AR Green assay buffer in the polypropylene plate, followed by transfer of 10 μL of each dilution to a 384-well black assay plate. Each well in the 384-well assay plate then received 5 μL of a 4× AR LBD GST dilution prepared in AR Green assay buffer for a final concentration of 5 nM. A 4× pre-mixture of Fl-labeled D11FxxLF peptide, Tb anti-GST anti-body, and DHT agonist, included at a concentration that corresponded to the EC_{60}−EC_{80} as determined from the agonist mode assay, was then added as a 5 μL aliquot to each well the for a final concentration of 500, 5, and 5 nM, respectively. The final assay volume was 20 μL. Appropriate controls included all components as above except: no antagonist (negative control); maximum antagonist (positive control); no AR LBD GST in an antagonist titration (negative control); and antagonist titration with no agonist (negative control). The plate was gently mixed, incubated at room temperature, and protected from light prior to TR-FRET measurement.

Z′-Factor Determinations. For the agonist mode assay, the *Z′*-factor was determined from 24-replicate wells containing maximal concentration of DHT or no agonist plus 5 nM AR LBD GST, 500 nM Fl-labeled D11FxxLF, and 5 nM Tb anti-GST antibody in AR Green assay buffer. For antagonist mode, the *Z′*-factor was determined from 24 replicate wells containing maximal concentration of CPA or no antagonist, followed by addition of 5 nM AR LBD GST plus 5 nM DHT, 500 nM Fl-labeled D11FxxLF, and 5 nM Tb anti-GST antibody. The assay was incubated at room temperature, and TR-FRET was measured at 1, 2, 4, 6, and 24 h. The *Z′* equation is

$$Z' = 1 - [(3\sigma_{c1} + 3\sigma_{c2})/|(\mu_{c1} - \mu_{c2})|]$$

where σ_{c1} and σ_{c2} are the standard deviations of the positive and negative control wells in the assay plate, respectively, and μ_{c1} and μ_{c2} are mean values for the positive and negative control wells in the assay plate, respectively (*43*). The reported *Z′*-factors are the average of three independent experiments.

Measurement of TR-FRET. TR-FRET was measured using a Tecan Ultra plate reader (Tecan, Durham, NC). The terbium donor was excited using a 340-nm excitation filter with a 30 nm bandwidth. The first (of four) terbium emission peaks is centered between 485−505 nm and overlaps with the

Table 1: Relative Binding Affinity of Panel of Ligands for Wild-Type AR or AR T877A[a]

ligand	IC_{50} (nM) wild-type AR	IC_{50} (nM) AR T877A	WT IC_{50}/ T877A IC_{50}
DHT	1.1 ± 0.04	1.3 ± 0.01	0.8
R1881	1.4 ± 0.2	1.3 ± 0.1	1.1
testosterone*	4.5 ± 0.2	2.6 ± 0.03	1.7
mifepristone*	66 ± 1	115 ± 5	0.6
estradiol*	240 ± 20	70 ± 3	3.4
spironolactone*	242 ± 8	8.9 ± 1.3	27
cyproterone acetate*	310 ± 0.5	32 ± 2	9.7
progesterone	560 ± 50	10 ± 0.5	56
hydroxyflutamide	2100 ± 200	144 ± 0.1	15
bicalutamide*	2300 ± 120	4500 ± 90	0.5
flutamide*	65200 ± 1300	9900 ± 400	6.6
cortisol	116000 ± 9800	7000 ± 300	17

[a] IC_{50} values represent ligand concentration required for 50% displacement of Fluormone AL Red from the receptor. Reported values were determined from two independent experiments. *, indicates difference between wild-type AR and AR T877A is statistically significant ($p < 0.05$).

excitation peak of fluorescein. TR-FRET values were calculated as the ratio of raw acceptor to donor intensities averaged from 10 excitations (flashes) per well and measured with a 100 μs post-excitation delay and 200 μs signal integration time. Background subtraction or crosstalk correction was not required. Using the stock "fluorescein" dichroic mirror supplied by Tecan, the acceptor signal was measured using a 520-nm filter (25-nm bandwidth), and the donor signal was measured using a 495-nm filter (10-nm bandwidth); (filter set PV003 from Chroma Technology Corp, Rockingham, VT). Binding curves were generated from the ratio of the 520 nm (acceptor) emission to the 495 nm (donor) emission (*y*-axis) versus the log of the concentration (*x*-axis). The data were fit using nonlinear regression with an equation for sigmoidal dose response (variable slope) in GraphPad Prism (GraphPad Software, Inc, San Diego, CA) or XLFit4 (IDBS, Guildford, UK). The statistical significance of the differences between WT AR and AR T877A was analyzed for Tables 1 and 3 using an unpaired t test or a more rigorous unpaired t test with Welch's correction (GraphPad Prism). The unpaired t test was used in data sets when the variances were not significantly different, and the unpaired t test with Welch's correction was used when the variances were significantly different, as determined in an F test. To determine the statistically significant differences between ligand relative binding affinity (Table 1) and ligand dose dependency for peptide interaction (Table 3), the IC_{50} values of Table 1 were compared with the corresponding EC_{50} or IC_{50} value of Table 3 with an unpaired t test using

Table 2: Fluorescein-Labeled Coregulator and Random Phage Display Peptides[a]

	P160 Family of Steroid Receptor Coactivators	
SRC1−1	KYSQTSHK**LVQLL**TTTAEQQL	NR box 1
SRC1−2	LTARHKI**LHRLL**QEGSPSD	NR box 2
SRC1−3	ESKDHQL**LRYLL**DKDEKDL	NR box 3
SRC1−4	GPQTPQAQQKSL**LQQLL**TE	NR box 4
SRC2−1	DSKGQTK**LLQLL**TTKSDQM	NR box 1
SRC2−2	LKEKHKI**LHRLL**QDSSSPV	NR box 2
SRC2−3	KKKENAL**LRYLL**DKDDTKD	NR box 3
SRC3−1	ESKGHKK**LLQLL**TCSSDDR	NR box 1
SRC3−2	LQEKHRI**LHKLL**QNGNSPA	NR box 2
SRC3−3	KKENNAL**LRYLL**DRDDPSD	NR box 3
	Other Important Coactivator Proteins	
CBP−1	AASKHKQ**LSELL**RGGSGSS	CREB binding protein, motif 1
TRAP220/DRIP−1	KVSQNPI**LTSLL**QITGNGG	TRAP220/DRIP205, motif 1
TRAP220/DRIP−2	NTKNHPM**LMNLL**KDNPAQD	TRAP220/DRIP205, motif 2
RIP140 L6	SHQKVTL**LQLLL**GHKNEEN	receptor interacting protein 140, motif 6
RIP140 L8	SFSKNGL**LSRLL**RQNQDSY	receptor interacting protein 140, motif 8
	PPAR-Specific Coactivator Proteins	
PGC1α	EAEEPSL**LKKLL**LAPANTQ	PPARγ coactivator protein 1α
PRIP/RAP250	VTLTSPL**LVNLL**QSDISAG	PPAR interacting protein 250
	Random Phage Display Peptides	
D22	LPYEGSL**LLKLL**RAPVEEV	resembles RIP140, PGC-1, DAX-1, SHP
C33	HVEMHPL**LMGLL**MESQWGA	resembles TRAP220, RIP140
EAB1	SSNHQSSR**LIELL**SR	tamoxifen-induced
EA2	SSKGVLWRMLAEPVSR	tamoxifen-induced
TA1	SRTLQLDWGTLYWSR	tamoxifen-induced
TB3	SSVASREWWVRELSR	tamoxifen-induced
	AR-Interactive Peptides	
AR(16−34)	SKTYRGA**FQNLF**QSVREVI	N-terminal AR sequence
ARA70	SRETSEK**FKLLF**QSYNVND	AR specific coactivator
D11 FxxLF	VESGSSR**FMQLF**MANDLLT	resembles GRIP1, SRC-1, AIB-1
	Corepressor Peptides	
SMRT ID1	GHQRVVT**LAQHISEVI**TQDYTRH	motif 1
SMRT ID2	HASTNMG**LEAIIRKAL**MGKYDQW	motif 2
NCoR ID1	RTHRLIT**LADHICQII**TQDFARN	motif 1
NCoR ID2 (short)	NLG**LEDIIRKAL**MG	motif 2

[a] The peptides containing interaction motifs (in bold) were labeled with fluorescein at the N-terminus. NR box, nuclear receptor interaction motif; PPAR, peroxisome proliferator-activated receptor; CBP, CREB binding protein; TRAP, thyroid hormone receptor associated protein; DRIP, vitamin D receptor interacting protein; RIP, receptor interacting protein; PRIP, PPAR interacting protein; AR, androgen receptor; DAX-1, dosage-sensitive sex reversal-adrenal hypoplasia congenital critical region on the X chromosome gene 1; SHP, short heterodimer partner; GRIP-1 glucocorticoid receptor-interacting protein 1; SRC-1, steroid receptor coactivator-1; AIB1, amplified in breast cancer 1; SMRT, silencing mediator for retinoid and thyroid hormone receptors; NCoR, nuclear corepressor; ID, interaction domain.

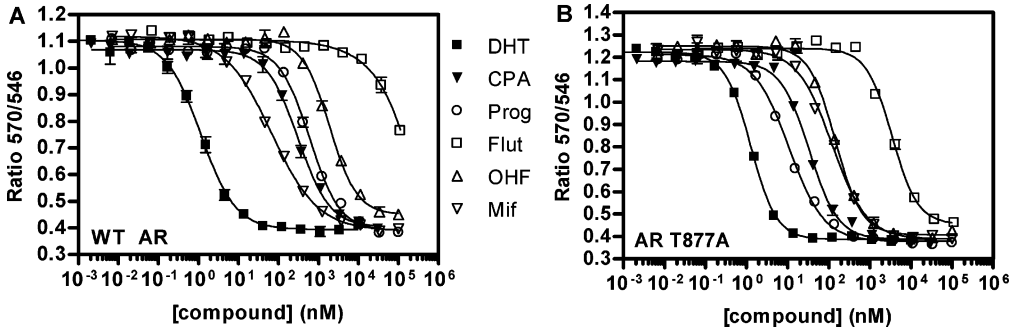

FIGURE 1: Relative binding affinities of selected ligands for AR WT versus AR T877A using a competitive binding assay. Increasing concentrations of each compound were incubated with 1 nM receptor, 10 nM Fluormone AL Red, and 5 nM Tb anti-GST antibody for 6 h prior to measurement of TR-FRET. Representative titrations of two independent experiments are shown for a subset of the ligands tested using WT AR (A) and AR T877A (B). Mif, mifepristone; Prog, progesterone; Flut, flutamide.

Table 3: Ligand EC_{50} or IC_{50} Values for Wild-Type AR or AR T877A in Agonist or Antagonist Mode[a]

agonist mode	EC_{50} (nM)		WT EC_{50}/
ligand	wild-type AR	AR T877A	T877A EC_{50}
R1881	2.6 ± 1.3	1.4 ± 1.0	1.9
DHT	3.2 ± 0.9	**3.3 ± 0.6**	1.0
testosterone	4.1 ± 1.1	2.9 ± 1.1	1.4
estradiol	**71 ± 19**	**12 ± 3.8**	5.9
spironolactone*	**100 ± 28**	7.7 ± 3.1	13
progesterone*	**267 ± 58**	**3.5 ± 1.2**	76
cortisol	**39300 ± 9700**	**1420 ± 23**	28
hydroxyflutamide*	**910 ± 190**	**34 ± 5.4**	27
cyproterone acetate	ND	ND	
mifepristone	ND	ND	

antagonist mode	IC_{50} (nM)		WT IC_{50}/
ligand	wild-type AR	AR T877A	T877A IC_{50}
cyproterone acetate*	322 ± 33	108 ± 18	3.0
mifepristone*	**210 ± 9.5**	**270 ± 7.1**	0.8
hydroxyflutamide	**519 ± 160**	159 ± 19	3.3
bicalutamide	2000 ± 720	**2560 ± 110**	0.8
flutamide*	**28000 ± 700**	**5600 ± 350**	5.0

[a] EC_{50} or IC_{50} values represent average ligand concentration (± standard error) for recruitment (agonist) or displacement (antagonist) of Fl-labeled D11FxxLF from receptor. All values were from 2 to 7 independent experiments. ND, not determined. *, indicates difference between wild-type AR and AR T877A is statistically significant ($p < 0.05$). Bold, indicates difference between Table 3 value and the corresponding ligand value in Table 1 is statistically significant ($p < 0.05$).

the mean value, standard error of each value, and the number (N) of replicates.

RESULTS

The ligand binding activity of the WT AR and AR T877A was assessed using a radioactive methyltrienolone (R1881) hydroxylapatite assay, to calculate the active concentration of receptor preparations, and by a TR-FRET-based competitive ligand binding assay. In this competitive assay, a Tb-labeled anti-GST antibody binds to the GST tag of the AR LBD, and a fluorescent AR ligand, Fluormone AL Red ("tracer"), binds to the ligand binding pocket of the receptor. When the Tb-labeled anti-GST antibody is excited, energy is transferred from the Tb to the fluorescent moiety on the tracer, allowing for detection of tracer binding to AR. Disruption of this FRET signal is then used to detect ligands that compete with the tracer for binding. When measured in a time-resolved mode, only the receptor-bound tracer is detected because of its proximity to the long lifetime Tb donor. The binding affinity (K_d) of Fluormone AL Red was measured as 12.3 ± 1.4 nM for WT AR LBD and 11.5 ± 1.3 nM for AR T877A LBD (data not shown). Thus, Fluormone AL Red could readily be used with both WT AR and AR T877A in a competitive binding assay to measure relative ligand binding affinities of common AR agonists and antagonists.

When increasing concentrations of ligand were used to displace Fluormone AL Red from the receptor, the agonists R1881, testosterone, and DHT all bound with low nanomolar ligand affinity to WT AR (Figure 1 or Table 1), in agreement with the relative binding affinities reported for these ligands (*2*). DHT and R1881 also bound with similar affinity to AR T877A. The ligands testosterone, estradiol, spironolactone, cyproterone acetate (CPA), progesterone, hydroxyflutamide (OHF), flutamide, and cortisol bound with higher affinity to the T877A mutant, compared to WT AR (Figure 1 and Table 1). Only mifepristone and bicalutamide bound with relative higher affinity to the WT AR than AR T877A (Table 1). The rank order affinity of ligands for WT AR was DHT ≈ R1881 > testosterone > mifepristone > estradiol ≈ spironolactone > CPA > progesterone >> OHF ≈ bicalutamide >> flutamide >> cortisol. These relative binding affinities were similar to those reported by Kemppainen et al. on a subset of these ligands using whole cell competitive binding assays (*2*). The rank order affinity of ligands for AR T877A was DHT ≈ R1881 > testosterone > spironolactone ≈ progesterone > CPA > estradiol > mifepristone > OHF >> bicalutamide > cortisol > flutamide. These T877A results are similar to the relative binding affinities of the ligands R1881, DHT, progesterone, CPA, and estradiol previously reported in LNCaP cells (*26*). Our results with progesterone, estradiol, OHF, and CPA agree with previous reports indicating that these ligands bind with higher affinity to AR T877A than WT AR (*26*, *29*, *32*). All ligands tested, except for bicalutamide, mifepristone, DHT, and R1881, bound with higher affinity to the mutant T877A receptor than WT AR, suggesting that the structural alterations in the ligand binding pocket generated from the change from the more bulky threonine to the smaller alanine results in a higher binding affinity for several agonists and antagonists.

To compare the interaction of the AR LBD versus the mutant T877A LBD with peptides derived from coactivator and corepressor proteins or from random phage display, a Tb donor-Fl acceptor methodology using TR-FRET was

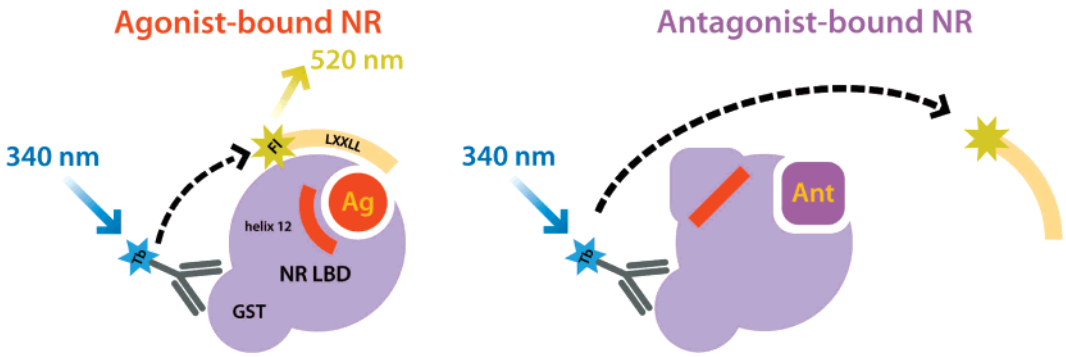

FIGURE 2: Principle of the peptide recruitment assay. The in vitro interaction assay is comprised of a GST-tagged nuclear receptor LBD, Tb anti-GST antibody, Fl-labeled LXXLL or FXXLF peptide, and a test ligand. When an agonist binds to the LBD, helix 12 adopts a conformation resulting in higher affinity of the receptor for the Fl-labeled LXXLL peptide. Light of 340 nm is used to excite the Tb label which in turn transfers energy to the Fl label on the peptide, yielding an increase in TR-FRET. Antagonist-occupied LBD has a less favorable conformation for interaction with the Fl-labeled LXXLL peptide resulting in no detectable TR-FRET. For simplicity, the AR protein is depicted as a monomer with one associated Tb anti-GST antibody transferring energy to one associated Fl-labeled coactivator peptide, but the exact stoichiometry and structure of this interaction is unknown. NR, nuclear receptor.

developed (Figure 2). Agonist-bound nuclear receptors adopt a favorable conformation around helix 12 in the LBD that results in higher affinity for the coactivator peptide, usually bearing an LXXLL or other similar interaction motif. When the Tb label on the anti-GST antibody is excited at 340 nm, energy is transferred to the Fl label on the associated coactivator peptide and detected as emission at 520 nm, resulting in a larger 520:495 emission ratio. Binding of antagonist to nuclear receptors causes a conformational change around helix 12 that precludes coactivator peptide binding, and no TR-FRET is detected. Gel filtration studies with purified AR T877A in the presence or absence of DHT suggested that the receptor is predominantly monomeric in agreement with crystal structure studies (*29*), and elution of AR T877A coincided with ligand binding activity as determined in a fluorescence polarization assay using Fluormone AL Red (data not shown).

The peptides tested (Table 2) were selected from known coregulator proteins or random phage display peptides bearing the coactivator LXXLL motif, AR-specific FXXLF motif, or the corepressor (CoRNR) box motif of L−X−X−I/H−I−X−X−X−I/L (*37*, *44*−*55*). The AR N-terminal sequence (AR 16−34) known to mediate an intradomain interaction with the LBD was also included. D11FxxLF has been shown to interact with AR comparable to AR coactivator motifs (*38*). The peptides included were chosen on literature predictions of what might interact with AR and other nuclear receptors as an initial broad screening panel. Each peptide was labeled at the N-terminus with Fl.

To determine which peptides interact with the receptor in a ligand-dependent manner, an initial peptide screen was conducted with constant amounts of AR LBD GST, Tb anti-GST antibody, Fl-labeled peptide, and excess amounts of DHT, OHF, or CPA or an equivalent volume of DMSO solvent (Figure 3). The peptides D11FxxLF, ARA70, and AR N-terminus gave the highest fold change in the presence of DHT compared to the no-ligand control as determined in the TR-FRET assay, and these three peptides were selected for further analysis in a peptide titration. The overall change in TR-FRET ratios for all peptides tested was similar for both WT AR (Figure 3A) and AR T877A (Figure 3B) suggesting that both receptors recruit these peptide motifs in a similar manner. Similar to previous reports, AR favored binding to peptides containing FXXLF motifs rather than LXXLL motifs (*31*, *38*, *40*, *56*, *57*). Our results with the AR N-terminal peptide also agreed well with those previously reported indicating that an N-terminus−LBD interaction occurs in the presence of agonist but is disrupted by antagonists such as OHF (*10*, *57*).

To choose the peptide that would provide the largest assay window, a peptide titration was conducted in the presence of WT AR LBD (Figure 4). All three peptides demonstrated agonist-dependent recruitment, as indicated by the larger TR-FRET ratio observed in the presence of DHT compared to CPA or no ligand (Figure 4). The increase in TR-FRET in the presence of no-ligand or CPA at high peptide concentrations is largely due to diffusion-enhanced FRET rather than nonspecific recruitment of the peptide to the receptor, as determined from peptide titrations done in the absence of receptor (Figure 4B) (*58*). These results also indicated that the largest assay window was between 250 and 500 nM of the Fl-labeled D11FxxLF peptide (see arrow; Figure 4B), and this peptide was selected for further studies. Ligand titrations using varying amounts of DHT, CPA, or DMSO solvent were conducted with constant amounts of AR, Tb anti-GST antibody, and either 250 or 500 nM Fl-labeled D11FxxLF (data not shown). The use of 500 nM Fl-labeled D11FxxLF gave the larger assay window (data not shown), and this concentration of peptide was used for subsequent experiments to examine ligand dose dependency on peptide recruitment. An estimate of peptide affinity indicated that Fl-labeled D11FxxLF bound with the highest affinity to DHT-occupied WT AR (Figure 5A) and AR T877A (Figure 5B). Use of higher concentrations of Fl-peptide to determine peptide-receptor affinities presents challenges because diffusion-enhanced FRET affects formation of an upper plateau, and therefore complete assessment of peptide affinity is difficult. Further comparisons of the effects of ligand on peptide recruitment to AR and AR T877A were conducted using ligand dose dependency studies.

To characterize the agonist dose dependency for Fl-labeled D11FxxLF recruitment to AR, ligand titrations were conducted in wells containing 5 nM AR LBD GST, 5 nM Tb anti-GST antibody, and 500 nM Fl-labeled D11FxxLF peptide. When DHT was titrated into the assay, the Fl-labeled D11FxxLF peptide was recruited to AR in a DHT-dependent

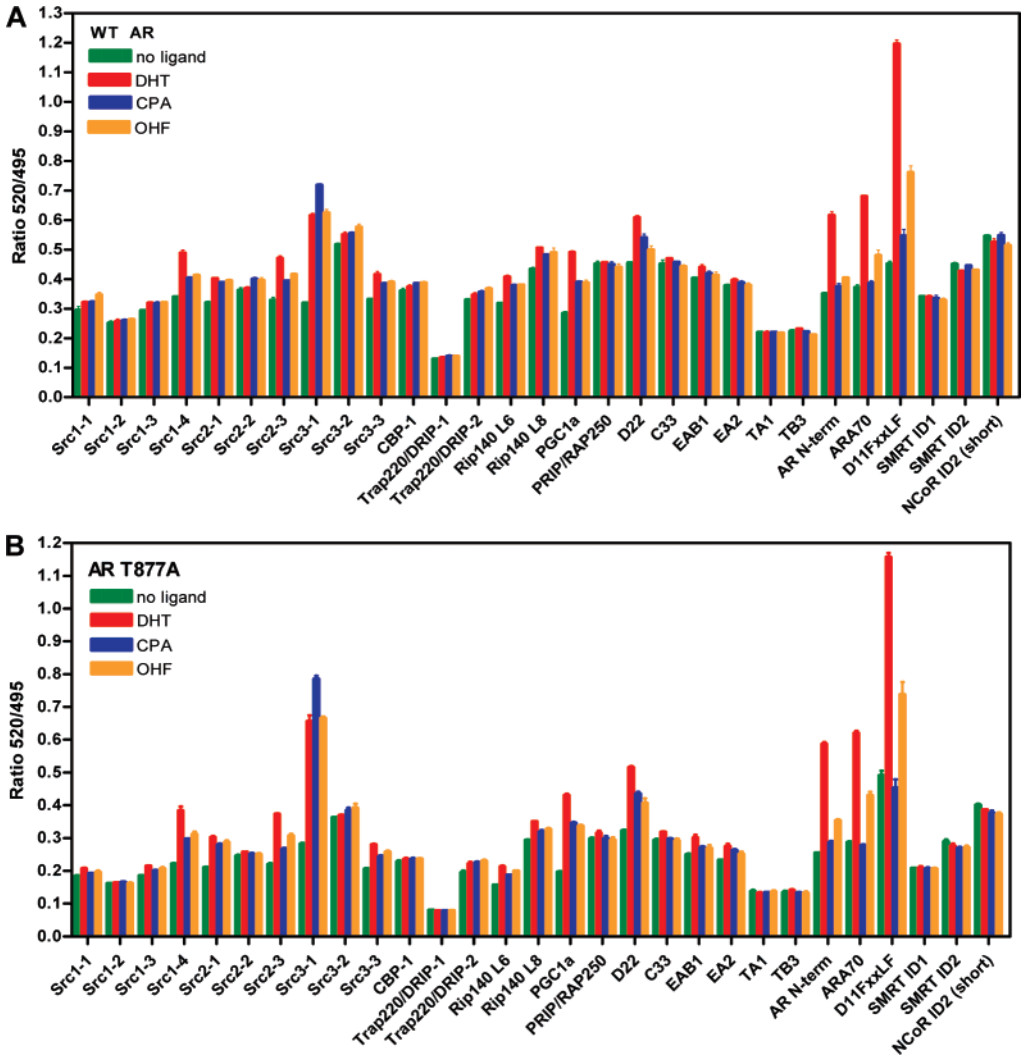

FIGURE 3: Screening of peptide panel with WT AR and mutant AR T877A in the TR-FRET recruitment assay. The TR-FRET ratio was measured after 4 h for reactions containing 20 nM AR LBD GST (A) or 20 nM AR T877A (B), 1 μM Fl-labeled peptide, 5 μM ligand (listed) or equivalent amount of DMSO solvent, and 5 nM Tb anti-GST antibody.

manner with an EC_{50} value of 4.6 nM at 4 h for the representative experiment shown (Figure 6) and an average of 3.2 $\pm$ 0.9 nM (Table 3). This EC_{50} was very stable at 2, 4, 6, and 24 h tested. The Hill Slope of the data fit (sigmoidal dose response, variable slope) indicates that positive cooperativity is occurring. This suggests that AR may be forming a dimer in the assay. FXXLF motifs have been shown to mediate intramolecular conformational changes prior to AR dimerization (*10*), and it is possible that D11FxxLF is facilitating an AR−AR interaction between the LBDs. Cooperativity could also be observed if ligand-induced receptor conformations lead to cooperative binding of multiple Tb anti-GST antibodies or a second Fl-peptide on the AR dimer. It should be noted that similar cooperative interactions are observed in a TR-FRET assay for PPARγ (*59*). The *Z*′-factor is a statistical parameter, often applied to high throughput applications, that measures both an assay signal dynamic range and the data variation of signal measurements (*43*). *Z*′-factors $\geq$0.5 indicate an excellent assay with high statistical reliability, and a value of 1 indicates a theoretically ideal assay with no variation (*43*). The average of the *Z*′-factor from three independent experiments was 0.78 at 4 h and averaged >0.7 at 2, 4, 6, and 24 h for WT AR, which indicated an excellent assay. The *Z*′-factor for DHT-mediated recruitment of Fl-labeled D11FxxLF to AR T877A from three independent experiments was 0.74 at 4 h and also averaged at least 0.7 at 2, 4, 6, and 24 h. The average EC_{80} for DHT ligand was 5 nM as calculated from multiple titrations and was used to design the antagonist response assay.

Experiments to quantitate the ligand dose dependency for Fl-labeled D11FxxLF recruitment to WT AR LBD (Figure 7A) versus AR T877A LBD (Figure 7B) in agonist mode indicated that several ligands (summarized in Table 3), such as progesterone, spironolactone, estradiol, OHF, and cortisol, have a lower EC_{50} value for the T877A mutant. Overall differences in the TR-FRET ratio observed with WT AR and the T877A mutant for ligands that yielded a maximal TR-FRET ratio (DHT and testosterone) versus ligands that resulted in an intermediate TR-FRET ratio (R1881, estradiol, spironolactone) are likely due to differences in receptor conformation and/or amount of complex formed (Figure 7). Slight fluctuations in maximal and minimal TR-FRET values between similar experiments can be observed from day to day due to changes in instrument gain settings, which is normal. Similar to Figure 6, the Hill slope indicates the presence of positive cooperativity especially in the presence of DHT, testosterone, and R1881, suggesting that ligand

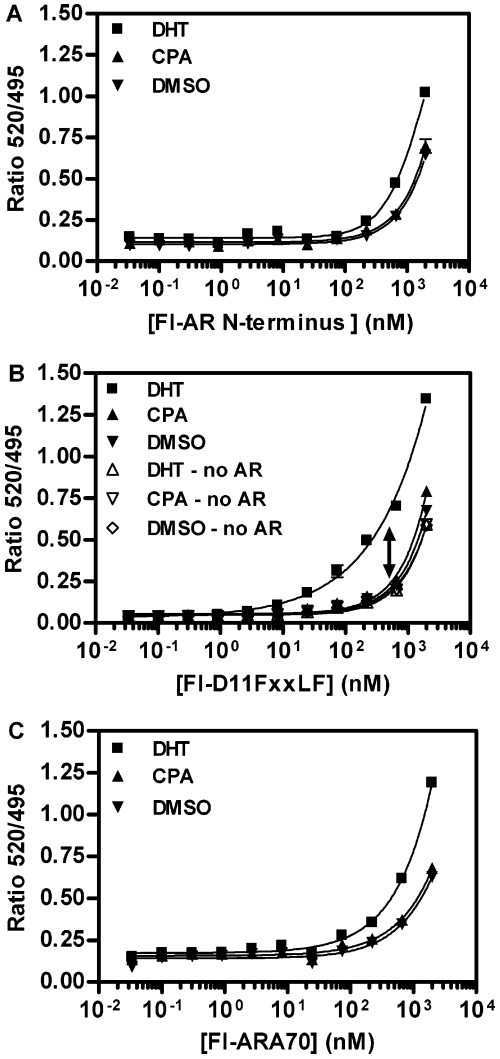

FIGURE 4: Titration of AR-interactive peptides in the TR-FRET recruitment assay. Fl-labeled AR N-terminus (A), D11FxxLF (B), or ARA70 (C) were serially diluted into assay buffer. A mixture of 20 nM AR LBD GST plus 5 μM ligand (listed) or equivalent DMSO solvent was added to each well, followed by 5 nM Tb anti-GST antibody. TR-FRET was measured at 4 h after incubation at room temperature. The arrow (B) indicates the potential assay window at 500 nM Fl-labeled D11FxxLF.

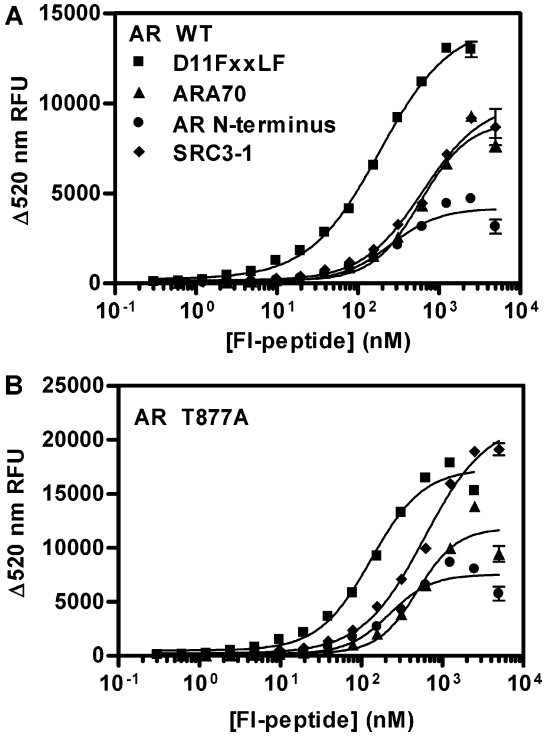

FIGURE 5: Estimation of peptide affinity for DHT-occupied WT AR and AR T877A. Fl-D11FxxLF, Fl-ARA70, Fl-AR N-terminus, or Fl-SRC3−1 were titrated into assays containing 5 μM DHT, 5 nM receptor, and 5 nM Tb anti-GST antibody. A parallel titration was run in the absence of receptor to correct for diffusion-enhanced FRET. The 520 emission for DHT-occupied receptor (minus the 520 emission in the absence of receptor) was plotted against peptide concentration. TR-FRET was read after 4 h at room temperature. The data is the mean of three replicates, and errors bars are SEM. (A) Data for WT AR. (B) Data for AR T877A. RFU, relative fluorescence units.

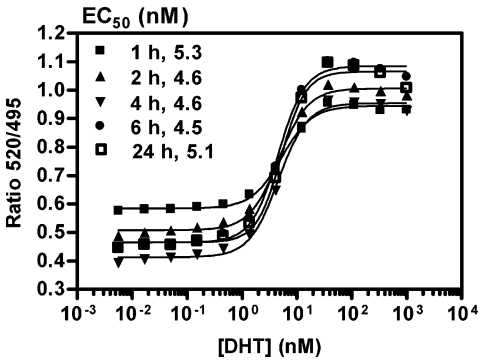

FIGURE 6: DHT-induced D11FxxLF recruitment to AR LBD GST. Increasing concentrations of DHT were incubated with 5 nM AR LBD GST, 500 nM Fl-labeled D11FxxLF, and 5 nM Tb anti-GST antibody. TR-FRET was measured after the times listed at room temperature. A representative experiment of three independent experiments is shown.

binding induces a receptor conformation that leads to AR dimerization and/or enhanced interactions between the receptor-bound Tb anti-GST antibody and Fl-peptide in the assay. Binding of estradiol and spironolactone to the WT AR does not appear to induce a receptor conformation that leads to this cooperativity. The rank order potency for ligand-mediated D11FxxLF−receptor interaction with WT AR was R1881 ≈ DHT ≈ testosterone > estradiol > spironolactone > progesterone > OHF >> cortisol. The rank order potency for AR T877A was R1881 > testosterone ≈ DHT ≈ progesterone > spironolactone > estradiol > OHF > cortisol. Although not all differences between WT AR and AR T877A in Table 1 and Table 3 were statistically significant (noted by asterisks), the differences were observed in multiple independent experiments, and therefore are scientifically important. For example, the 6-fold difference between EC_{50} values for WT AR and AR T877A in the presence of estradiol, summarized in Table 3, was observed in each of three independent experiments. The standard error (from the average of these three independent experiments) that arises from day-to-day instrument gain settings, slight variation in pipetting between users, and other usual experimental error precluded the assignment of statistical significance for every ligand (p value was 0.0522 for estradiol in Table 3). However, a very reproducible trend was found in these experiments.

For estradiol, progesterone, cortisol, and OHF, the increase in ligand binding affinity for AR T877A ranged from 3- to 56-fold (Table 1), but the improved potency for these ligands mediating Fl-D11xxLF interaction with AR T877A ranged

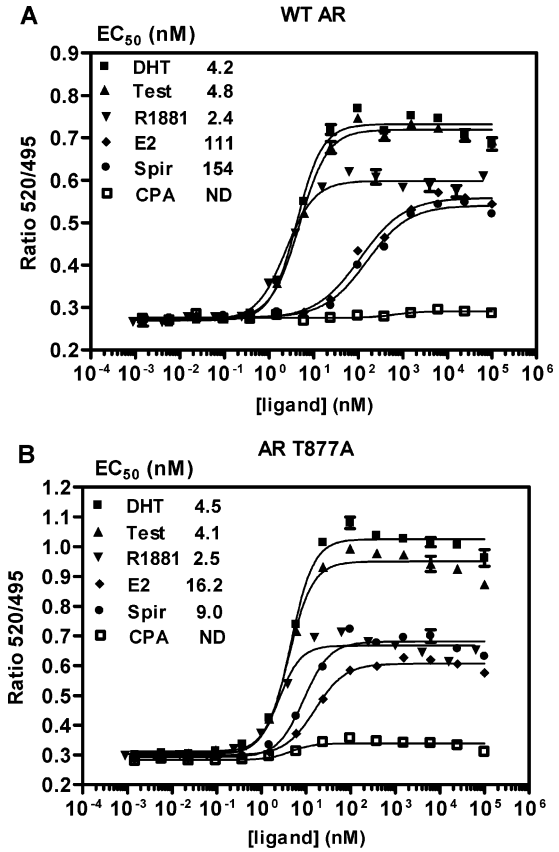

FIGURE 7: Differential ligand potency for D11FxxLF recruitment to AR WT versus AR T877A mutant in the TR-FRET recruitment assay. Increasing concentrations of ligand (listed) were incubated with 5 nM AR LBD GST (A) or 5 nM AR T877A LBD GST mutant (B) plus 500 nM Fl-labeled D11FxxLF and 5 nM Tb anti-GST antibody. TR-FRET was measured after a 4 h incubation at room temperature. A representative experiment of 3−7 independent experiments is shown. Test, testosterone; E2, estradiol; Spir, spironolactone.

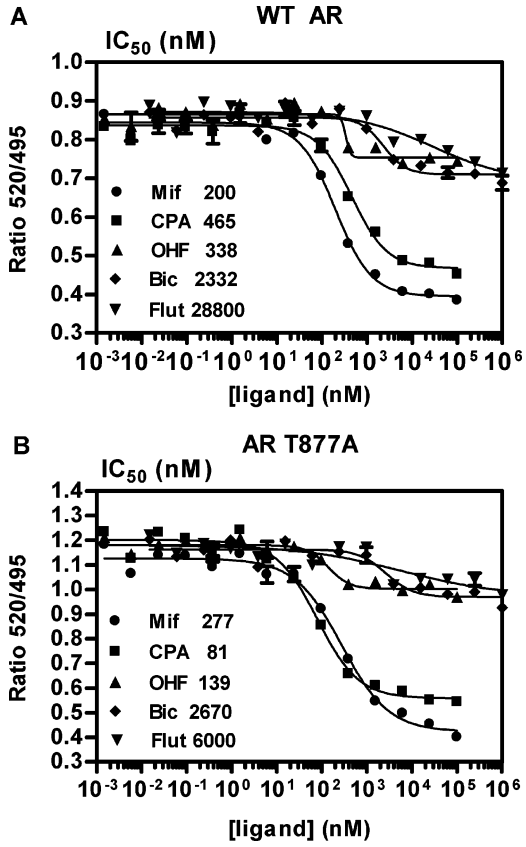

FIGURE 8: Antagonist-induced displacement of D11FxxLF from AR LBD GST versus AR T877A mutant. Increasing concentrations of antagonist (listed) were incubated with 5 nM AR LBD GST (A) or 5 nM AR T877A LBD GST (B) followed by addition of 500 nM Fl-labeled D11FxxLF, 5 nM Tb anti-GST antibody, and 5 nM DHT. The assay was incubated at room temperature, and TR-FRET was measured at 4 h. These results are from 2 to 7 independent experiments with the listed ligands. Mif, mifepristone; Bic, bicalutamide; Flut, flutamide.

from 6- to 76-fold (Table 3). If the Fl-labeled D11FxxLF concentration is at excess but not at saturating levels (approximately 10 times the affinity estimation), the ligand dose dependency value for peptide recruitment or displacement likely includes multiple equilibrium events involving the ligand affinity for the receptor, the equilibrium between ligand-induced receptor conformational states, and the peptide affinity for the ligand-occupied receptor, and therefore this dose dependency value may not exactly equal the ligand affinity value. To determine whether this was the case, further statistical analysis was conducted to compare the dose dependency value of Table 3 with the corresponding ligand IC_{50} value in Table 1. Several dose dependency values (shown in bold, Table 3) indicated a statistically significant difference from Table 1. Although the lower dose dependency values observed for AR T877A in Table 3 likely reflect the increased ligand affinity found in Table 1 (see ratio columns in Tables 1 and 3), for those ligands shown in bold other factors such as the peptide affinity and rates of ligand-induced receptor conformational change appear to affect the EC_{50} for peptide recruitment or IC_{50} for peptide displacement, as indicated by the statistically significant differences between ligand relative binding affinity and ligand dose dependency for peptide interaction. These results, summarized in Tables 1 and 3, suggest that differences in AR T877A ligand potency, compared to WT AR, are a combination of both the effect on ligand affinity for the receptor and the ligand dose dependency for peptide interaction with the receptor.

The ability of the AR antagonists CPA, OHF, flutamide, bicalutamide, and mifepristone to disrupt the DHT-mediated Fl-labeled D11FxxLF−AR LBD interaction in a dose-dependent manner was tested for both WT AR and AR T877A (Figure 8). In antagonist mode, 5 nM AR LBD GST was added to antagonist titrations followed by addition of 5 nM Tb anti-GST antibody, 500 nM Fl-labeled D11FxxLF, and 5 nM DHT. Recruitment of Fl-labeled D11FxxLF to either WT AR (Figure 8A) or AR T877A (Figure 8B) in the presence of DHT agonist was disrupted to a greater extent by CPA and mifepristone, compared to flutamide, OHF, and bicalutamide. Increasing concentrations of CPA disrupted the DHT-induced interaction between AR LBD GST and Fl-labeled D11FxxLF with an IC_{50} value of 465 nM (Figure 8A; summarized in Table 3) and a Z' of ≥ 0.5 after the 4 h incubation. Saturating amounts of CPA resulted in displacement of D11FxxLF peptide from AR with a bottom plateau of ~0.5 FRET ratio (Figure 8A). However, high concentrations of OHF and bicalutamide resulted in a bottom plateau near ~0.7 FRET ratio. In the case of OHF, this smaller fold-change is likely due to the higher affinity between OHF-occupied AR and D11FxxLF compared to CPA, as suggested by the difference in the maximal TR-FRET ratio observed

in the presence of these two ligands (Figure 3). Another factor that could influence the TR-FRET ratio observed in the antagonist-induced displacement of Fl-labeled D11FxxLF is the difference in receptor conformation. Higher concentrations of flutamide to better define a bottom plateau could not be tested due to solubility limitations. Our results showing mifepristone as a strong AR antagonist agree with the anti-androgen effects of this ligand on AR reporter gene expression previously reported (*41*). Although the relative binding affinity of OHF for AR T877A was similar to mifepristone according to IC_{50} values (Table 1), mifepristone elicited a more complete disruption of the D11FxxLF−AR LBD interaction, suggesting its usefulness as an anti-androgen. Our findings indicate that CPA- or mifepristone-induced displacement of D11FxxLF would be useful for comparisons to other antagonists and unknown test compounds, if this methodology is used to screen ligands. The average *Z*′-factor (*43*) for the CPA-induced disruption of the DHT-mediated WT AR complex with Fl-labeled D11FxxLF, as determined from three independent experiments, was 0.51 at 4 h and averaged at least 0.5 at 2, 4, and 6 h which indicated an excellent reproducible methodology. Similarly, the *Z*′-factor for AR T877A in the antagonist mode from 3 independent experiments was 0.57 at 4 h and also averaged >0.5 at 2, 4, and 6 h.

Although CPA has been shown previously to behave as an agonist for AR T877A (*34*, *35*, *41*), in multiple experiments CPA consistently antagonized the interaction between Fl-labeled D11FxxLF and AR T877A. Since these peptides are expected to be sensitive to different receptor conformations, we explored whether another peptide might recognize an agonistic AR T877A conformation induced by CPA. As shown in Figure 9, CPA was 10-fold more potent and OHF was 20-fold more potent in inducing an interaction between AR T877A and Fl-labeled SRC3−1, compared to WT AR. This effect of CPA is similar to the results of Berrevoets et al. who observed partial agonistic activity on wild-type AR gene transactivation and more potent CPA effects on AR T877A in LNCaP cells (*35*). Although SRC3−1 is an LXXLL-containing peptide, overexpression of SRC3 has been detected in LNCaP cells, suggesting a correlation with prostate cancer signaling (*25*). These results highlight the usefulness of employing several peptides, such as D11FxxLF and SRC3−1, to determine the effect of ligand-induced receptor conformations and to enhance the biological relevance of results observed with purified LBDs and short peptides in vitro.

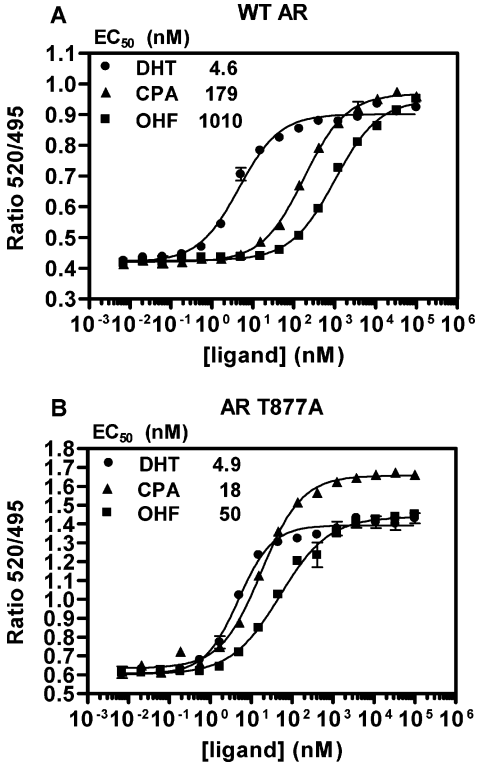

FIGURE 9: Ligand-induced SRC3−1 recruitment to AR LBD GST versus AR T877A mutant. Increasing concentrations of DHT, CPA, or OHF were incubated with 5 nM AR LBD GST (A) or 5 nM AR T877A LBD GST (B), 500 nM Fl-labeled SRC3−1, and 5 nM Tb anti-GST antibody. TR-FRET was measured after a 4 h incubation at room temperature.

DISCUSSION

Our results indicate that WT AR and AR T877A are characterized by differential ligand binding affinities and ligand dose dependency for peptide recruitment. Using a competitive binding assay, we observed that several ligands tested except for mifepristone and bicalutamide bound with higher affinity to AR T877A than to WT AR. In particular, progesterone, estradiol, cortisol, and OHF bound with higher affinity to AR T877A than WT AR, similar to other reports (*30*, *32*, *33*), and we also observed higher affinity for the mutant with other ligands such as spironolactone, CPA, and flutamide. DHT and R1881 bound with similar affinity to both WT AR and AR T877A. Our results indicate that many ligands can bind with higher affinity to the AR T877A mutation, potentially due to the larger binding pocket, compared to WT AR.

D11FxxLF is a random phage display peptide that resembles the SRC family of coactivator proteins in its flanking sequences but also has the FXXLF motif found in the AR N-terminal interaction domain and AR-specific coactivators. In this regard, D11FxxLF is a biological mimic of the N-terminal and SRC coactivator interactions with the AR LBD. In the agonist-mediated D11FxxLF recruitment studies (Table 3), we found that the agonists DHT, testosterone, and R1881 had similar EC_{50} values for D11FxxLF interaction with either WT AR or AR T877A. Estradiol, spironolactone, and progesterone all exhibited increased potency for D11FxxLF recruitment to AR T877A, compared to WT AR. Also of note, AR T877A responded to cortisol as an agonist with increased potency in recruitment of Fl-labeled D11FxxLF, compared to WT AR, similar to previous reports by Steketee and colleagues (*30*). The effect of the T877A mutation on both ligand affinity and dose dependency for D11FxxLF recruitment is encompassed in the ligand EC_{50} values observed in the peptide recruitment assay, which is a composite value reflecting multiple equilibrium events between ligand affinity for the receptor, receptor conformational states, and peptide affinity for the receptor. Although overall levels of D11FxxLF recruitment to WT AR or AR T877A were similar in the presence of excess ligand (Figure 3), the observed increase in ligand affinity and related increase in ligand potency for D11FxxLF recruitment to AR T877A for ligands such as estrogen, progesterone, cortisol, spironolactone, and OHF may explain in part the upregulation

of gene expression and cell growth rates previously reported in LNCaP cells (*22*).

In our studies, we wanted to examine if antagonists such as OHF and CPA would behave as agonists in mediating recruitment of peptides to AR T877A versus WT AR. When OHF was used in the TR-FRET assay in antagonist mode (Figure 8), the level of displacement of the DHT-mediated D11FxxLF peptide complex with either WT AR or AR T877A was marginal, indicating that OHF was inducing a receptor conformational state with substantial affinity for the D11FxxLF peptide. However, when OHF was used in the TR-FRET assay in agonist mode (see Table 3), it exhibited 27-fold increased potency as an agonist for AR T877A in the recruitment of D11FxxLF, as compared to WT AR, verifying that OHF was inducing a partial agonist receptor conformation capable of interaction with D11FxxLF. This result agrees with previous reports describing partial agonist activity of OHF on WT AR in reporter assays and receptor conformation studies (*60*, *61*). Previous reports have indicated that AR T877A responds to OHF as an agonist in gene transactivation or cell growth studies (*34*, *35*). The 15-fold increase in OHF affinity (see Table 1) for AR T877A compared to WT AR coupled with the 27-fold increased potency in the D11FxxLF recruitment to AR T877A compared to WT AR suggests that both effects may contribute to the agonist activity induced by OHF on AR T877A. CPA consistently behaved as an antagonist in the displacement of D11FxxLF from either WT AR or AR T877A. However, CPA had agonist activity and was characterized by increased potency in the recruitment of SRC3−1 to AR T877A compared to WT AR, indicating that different peptides are able to recognize the CPA-induced receptor conformation with altered affinity. Flutamide and bicalutamide exhibited only intermediate displacement of D11FxxLF from either WT AR or AR T877A, suggesting that these ligands possessed only partial antagonist activity in the displacement of D11FxxLF from the receptor. These results suggest that SRC3−1 might be more biologically relevant as a peptide sensor to discern the agonist effects of usual antagonists such as CPA and OHF.

Mifepristone resulted in the most complete displacement of D11FxxLF from both WT AR and AR T877A. Our results agree in part with previous findings that described mifepristone as a potential anti-androgen for prostate cancer therapy (*41*, *62*). Similar to Song and co-workers who detected mifepristone inhibition of R1881-mediated AR interactions with coactivators, TIF2 and β-catenin (*41*), we also observed mifepristone-induced disruption of DHT-mediated complex formation of both D11FxxLF−AR LBD and D11FxxLF−AR T877A LBD. The antagonist effect of mifepristone on both WT AR and AR T877A and its ability to completely displace D11FxxLF similar to CPA highlight its potential usefulness as a prostate cancer therapeutic. Song et al. also described an interaction between AR and the interaction domains of corepressors, NCoR and SMRT, with mifepristone mediating a stronger interaction than OHF, CPA, or bicalutamide, as determined by mammalian two-hybrid and co-immunoprecipitation studies (*41*). Cheng et al. also showed a direct interaction between the NCoR interaction domain and AR that could inhibit DHT-mediated transcription (*63*). We tested four interaction motifs from NCoR and SMRT (Table 2), including an extended version of the NCoR ID2 peptide, in the presence of DHT, R1881, CPA, OHF, bicalutamide, and mifepristone and also in the absence of any ligand for both WT AR and AR T877A and observed only a very low-level mifepristone-induced interaction of SMRT ID2 with WT AR and AR T877A (data not shown). Our results may differ because we used a corepressor peptide in an in vitro assay versus the larger corepressor protein domains in cellular studies where other bridging factors may enhance this interaction.

The fluorescence-based methodologies described here offer several advantages for high throughput screening. The competitive binding assay using Fluormone AL Red provides a method to compare relative ligand binding affinities for AR and mutations thereof in a solution-based format, without the need to use radioactivity or to separate bound from free ligand. In this regard, the tracer displacement approach is useful as a primary screen of compound libraries to identify potential ligands. The TR-FRET peptide recruitment format would be particularly useful as a secondary screen to then differentiate ligands as agonists or antagonists of the D11FxxLF−AR interaction. Similar TR-FRET formats have been employed for other coactivator peptide−nuclear receptor interactions (*59*, *64*). In our methodology, the use of a Tb chelate anti-GST antibody provides a means to fluorescently label any GST-tagged protein. The ability of the luminescent lanthanide, Tb, to pair with common acceptors such as Fl (*65*, *66*) enables the use of several different peptides, easily labeled with these fluorophores, in a panel to examine multiple peptide−AR interactions. Although not encountered in these studies, it should be noted that false negatives may occur if a test compound inactivates the receptor or directly causes the antibody or peptide to be displaced. Our TR-FRET assays were also tolerant of solvents commonly used in pharmaceutical libraries such as methanol, ethanol, and DMSO (data not shown), indicating that these assays are amenable to high throughput screening. Therefore, this format provides a useful methodology to build a panel of assays to examine multiple nuclear receptor LBD−coregulator peptide interactions.

In conclusion, our studies indicate that AR T877A is characterized by increased ligand binding affinity and increased ligand potency in peptide recruitment for several ligands such as estradiol, progesterone, spironolactone, OHF, and CPA, which may explain in part how AR T877A is activated by progesterone, estrogen, and anti-androgens during prostate cancer treatment. Recent studies have indicated that FXXLF-containing peptides may be able to function as antagonists themselves for ligand-dependent or ligand-independent AR-mediated gene transcription (*57*). Our methodologies could be used to further probe the biology of AR-peptide interactions to find peptide antagonists for use as new therapeutics and also to screen unknown compounds as agonists, antagonists, or partial modulators based on their ability to either promote or disrupt peptide interactions with AR.

ACKNOWLEDGMENT

The authors thank Nathan Spangler, Mark Maffitt, and Deborah Stafslien for technical assistance; Kurt Vogel, Richard Somberg, and Tina Hallis for comments on the manuscript; Greg Parker and Augustine Agado for assistance

with graphics; and Bill Checovich for assistance with statistical analysis.

REFERENCES

1. Gronemeyer, H., Gustafsson, J. A., and Laudet, V. (2004) Principles for modulation of the nuclear receptor superfamily, *Nat. Rev. Drug Discov. 3*, 950−964.
2. Kemppainen, J. A., Lane, M. V., Sar, M., and Wilson, E. M. (1992) Androgen receptor phosphorylation, turnover, nuclear transport, and transcriptional activation. Specificity for steroids and antihormones, *J. Biol. Chem. 267*, 968−974.
3. Berrevoets, C. A., Doesburg, P., Steketee, K., Trapman, J., and Brinkmann, A. O. (1998) Functional interactions of the AF-2 activation domain core region of the human androgen receptor with the amino-terminal domain and with the transcriptional coactivator TIF2 (transcriptional intermediary factor 2), *Mol. Endocrinol. 12*, 1172−1183.
4. Yeh, S., and Chang, C. (1996) Cloning and characterization of a specific coactivator, ARA70, for the androgen receptor in human prostate cells, *Proc. Natl. Acad. Sci. U.S.A. 93*, 5517−5521.
5. Fujimoto, N., Yeh, S., Kang, H. Y., Inui, S., Chang, H. C., Mizokami, A., and Chang, C. (1999) Cloning and characterization of androgen receptor coactivator, ARA55, in human prostate, *J. Biol. Chem. 274*, 8316−8321.
6. Kang, H. Y., Yeh, S., Fujimoto, N., and Chang, C. (1999) Cloning and characterization of human prostate coactivator ARA54, a novel protein that associates with the androgen receptor, *J. Biol. Chem. 274*, 8570−8576.
7. Estebanez-Perpina, E., Moore, J. M., Mar, E., Delgado-Rodrigues, E., Nguyen, P., Baxter, J. D., Buehrer, B. M., Webb, P., Fletterick, R. J., and Guy, R. K. (2005) The molecular mechanisms of coactivator utilization in ligand-dependent transactivation by the androgen receptor, *J. Biol. Chem. 280*, 8060−8068.
8. He, B., Kemppainen, J. A., Voegel, J. J., Gronemeyer, H., and Wilson, E. M. (1999) Activation function 2 in the human androgen receptor ligand binding domain mediates interdomain communication with the NH(2)-terminal domain, *J. Biol. Chem. 274*, 37219−37225.
9. He, B., Kemppainen, J. A., and Wilson, E. M. (2000) FXXLF and WXXLF sequences mediate the NH2-terminal interaction with the ligand binding domain of the androgen receptor, *J. Biol. Chem. 275*, 22986−22994.
10. Schaufele, F., Carbonell, X., Guerbadot, M., Borngraeber, S., Chapman, M. S., Ma, A. A., Miner, J. N., and Diamond, M. I. (2005) The structural basis of androgen receptor activation: intramolecular and intermolecular amino-carboxy interactions, *Proc. Natl. Acad. Sci. U.S.A. 102*, 9802−9807.
11. Gaddipati, J. P., McLeod, D. G., Heidenberg, H. B., Sesterhenn, I. A., Finger, M. J., Moul, J. W., and Srivastava, S. (1994) Frequent detection of codon 877 mutation in the androgen receptor gene in advanced prostate cancers, *Cancer Res. 54*, 2861−2864.
12. Suzuki, H., Sato, N., Watabe, Y., Masai, M., Seino, S., and Shimazaki, J. (1993) Androgen receptor gene mutations in human prostate cancer, *J. Steroid Biochem. Mol. Biol. 46*, 759−765.
13. Culig, Z., Klocker, H., Bartsch, G., and Hobisch, A. (2002) Androgen receptors in prostate cancer, *Endocr. Relat. Cancer 9*, 155−170.
14. Taplin, M. E., Bubley, G. J., Shuster, T. D., Frantz, M. E., Spooner, A. E., Ogata, G. K., Keer, H. N., and Balk, S. P. (1995) Mutation of the androgen-receptor gene in metastatic androgen-independent prostate cancer, *N. Engl. J. Med. 332*, 1393−1398.
15. Jemal, A., Murray, T., Ward, E., Samuels, A., Tiwari, R. C., Ghafoor, A., Feuer, E. J., and Thun, M. J. (2005) Cancer statistics, 2005, *CA Cancer J. Clin. 55*, 10−30.
16. Taplin, M. E., Bubley, G. J., Ko, Y. J., Small, E. J., Upton, M., Rajeshkumar, B., and Balk, S. P. (1999) Selection for androgen receptor mutations in prostate cancers treated with androgen antagonist, *Cancer Res. 59*, 2511−2515.
17. Visakorpi, T., Hyytinen, E., Koivisto, P., Tanner, M., Keinanen, R., Palmberg, C., Palotie, A., Tammela, T., Isola, J., and Kallioniemi, O. P. (1995) In vivo amplification of the androgen receptor gene and progression of human prostate cancer, *Nat. Genet. 9*, 401−406.
18. Linja, M. J., Savinainen, K. J., Saramaki, O. R., Tammela, T. L., Vessella, R. L., and Visakorpi, T. (2001) Amplification and overexpression of androgen receptor gene in hormone-refractory prostate cancer, *Cancer Res. 61*, 3550−3555.
19. Linja, M. J., and Visakorpi, T. (2004) Alterations of androgen receptor in prostate cancer, *J. Steroid Biochem. Mol. Biol. 92*, 255−264.
20. Culig, Z., Hobisch, A., Cronauer, M. V., Cato, A. C., Hittmair, A., Radmayr, C., Eberle, J., Bartsch, G., and Klocker, H. (1993) Mutant androgen receptor detected in an advanced-stage prostatic carcinoma is activated by adrenal androgens and progesterone, *Mol. Endocrinol. 7*, 1541−1550.
21. McDonald, S., Brive, L., Agus, D. B., Scher, H. I., and Ely, K. R. (2000) Ligand responsiveness in human prostate cancer: structural analysis of mutant androgen receptors from LNCaP and CWR22 tumors, *Cancer Res. 60*, 2317−2322.
22. Veldscholte, J., Ris-Stalpers, C., Kuiper, G. G., Jenster, G., Berrevoets, C., Claassen, E., van Rooij, H. C., Trapman, J., Brinkmann, A. O., and Mulder, E. (1990) A mutation in the ligand binding domain of the androgen receptor of human LNCaP cells affects steroid binding characteristics and response to antiandrogens, *Biochem. Biophys. Res. Commun. 173*, 534−540.
23. Linja, M. J., Porkka, K. P., Kang, Z., Savinainen, K. J., Janne, O. A., Tammela, T. L., Vessella, R. L., Palvimo, J. J., and Visakorpi, T. (2004) Expression of androgen receptor coregulators in prostate cancer, *Clin. Cancer Res. 10*, 1032−1040.
24. Gregory, C. W., He, B., Johnson, R. T., Ford, O. H., Mohler, J. L., French, F. S., and Wilson, E. M. (2001) A mechanism for androgen receptor-mediated prostate cancer recurrence after androgen deprivation therapy, *Cancer Res. 61*, 4315−4319.
25. Gnanapragasam, V. J., Leung, H. Y., Pulimood, A. S., Neal, D. E., and Robson, C. N. (2001) Expression of RAC 3, a steroid hormone receptor co-activator in prostate cancer, *Br. J. Cancer. 85*, 1928−1936.
26. Veldscholte, J., Berrevoets, C. A., Ris-Stalpers, C., Kuiper, G. G., Jenster, G., Trapman, J., Brinkmann, A. O., and Mulder, E. (1992) The androgen receptor in LNCaP cells contains a mutation in the ligand binding domain which affects steroid binding characteristics and response to antiandrogens, *J. Steroid Biochem. Mol. Biol. 41*, 665−669.
27. Suzuki, H., Akakura, K., Komiya, A., Aida, S., Akimoto, S., and Shimazaki, J. (1996) Codon 877 mutation in the androgen receptor gene in advanced prostate cancer: relation to antiandrogen withdrawal syndrome, *Prostate 29*, 153−158.
28. Matias, P. M., Donner, P., Coelho, R., Thomaz, M., Peixoto, C., Macedo, S., Otto, N., Joschko, S., Scholz, P., Wegg, A., Basler, S., Schafer, M., Egner, U., and Carrondo, M. A. (2000) Structural evidence for ligand specificity in the binding domain of the human androgen receptor. Implications for pathogenic gene mutations, *J. Biol. Chem. 275*, 26164−26171.
29. Sack, J. S., Kish, K. F., Wang, C., Attar, R. M., Kiefer, S. E., An, Y., Wu, G. Y., Scheffler, J. E., Salvati, M. E., Krystek, S. R., Jr., Weinmann, R., and Einspahr, H. M. (2001) Crystallographic structures of the ligand-binding domains of the androgen receptor and its T877A mutant complexed with the natural agonist dihydrotestosterone, *Proc. Natl. Acad. Sci. U.S.A. 98*, 4904−4909.
30. Steketee, K., Timmerman, L., Ziel-van der Made, A. C., Doesburg, P., Brinkmann, A. O., and Trapman, J. (2002) Broadened ligand responsiveness of androgen receptor mutants obtained by random amino acid substitution of H874 and mutation hot spot T877 in prostate cancer, *Int. J. Cancer. 100*, 309−317.
31. He, B., Gampe, R. T., Jr., Kole, A. J., Hnat, A. T., Stanley, T. B., An, G., Stewart, E. L., Kalman, R. I., Minges, J. T., and Wilson, E. M. (2004) Structural basis for androgen receptor interdomain and coactivator interactions suggests a transition in nuclear receptor activation function dominance, *Mol. Cell. 16*, 425−438.
32. Ai, N., DeLisle, R. K., Yu, S. J., and Welsh, W. J. (2003) Computational models for predicting the binding affinities of ligands for the wild-type androgen receptor and a mutated variant associated with human prostate cancer, *Chem. Res. Toxicol. 16*, 1652−1660.
33. Bohl, C. E., Miller, D. D., Chen, J., Bell, C. E., and Dalton, J. T. (2005) Structural basis for accommodation of nonsteroidal ligands in the androgen receptor, *J. Biol. Chem. 280*, 37747−37754.
34. Wilding, G., Chen, M., and Gelmann, E. P. (1989) Aberrant response in vitro of hormone-responsive prostate cancer cells to antiandrogens, *Prostate 14*, 103−115.
35. Berrevoets, C. A., Veldscholte, J., and Mulder, E. (1993) Effects of antiandrogens on transformation and transcription activation of wild-type and mutated (LNCaP) androgen receptors, *J. Steroid Biochem. Mol. Biol. 46*, 731−736.

36. Vanderschueren, D., Vandenput, L., Boonen, S., Lindberg, M. K., Bouillon, R., and Ohlsson, C. (2004) Androgens and bone, *Endocr. Rev. 25*, 389−425.
37. He, B., Minges, J. T., Lee, L. W., and Wilson, E. M. (2002) The FXXLF motif mediates androgen receptor-specific interactions with coregulators, *J. Biol. Chem. 277*, 10226−10235.
38. He, B., and Wilson, E. M. (2003) Electrostatic modulation in steroid receptor recruitment of LXXLL and FXXLF motifs, *Mol. Cell. Biol. 23*, 2135−2150.
39. Dubbink, H. J., Hersmus, R., Pike, A. C., Molier, M., Brinkmann, A. O., Jenster, G., and Trapman, J. (2006) Androgen Receptor Ligand-Binding Domain Interaction and Nuclear Receptor Specificity of FXXLF and LXXLL motifs as determined by L/F swapping, *Mol. Endocrinol. 20*, 1742−1755.
40. Hur, E., Pfaff, S. J., Payne, E. S., Gron, H., Buehrer, B. M., and Fletterick, R. J. (2004) Recognition and accommodation at the androgen receptor coactivator binding interface, *PLoS Biol. 2*, E274.
41. Song, L. N., Coghlan, M., and Gelmann, E. P. (2004) Antiandrogen effects of mifepristone on coactivator and corepressor interactions with the androgen receptor, *Mol. Endocrinol. 18*, 70−85.
42. He, B., Gampe, R. T., Jr., Hnat, A. T., Faggart, J. L., Minges, J. T., French, F. S., and Wilson, E. M. (2006) Probing the functional link between androgen receptor coactivator and ligand-binding sites in prostate cancer and androgen insensitivity, *J. Biol. Chem. 281*, 6648−6663.
43. Zhang, J. H., Chung, T. D., and Oldenburg, K. R. (1999) A Simple Statistical Parameter for Use in Evaluation and Validation of High Throughput Screening Assays, *J. Biomol. Screen 4*, 67−73.
44. Onate, S. A., Tsai, S. Y., Tsai, M. J., and O'Malley, B. W. (1995) Sequence and characterization of a coactivator for the steroid hormone receptor superfamily, *Science 270*, 1354−1357.
45. Voegel, J. J., Heine, M. J., Zechel, C., Chambon, P., and Gronemeyer, H. (1996) TIF2, a 160 kDa transcriptional mediator for the ligand-dependent activation function AF-2 of nuclear receptors, *EMBO J. 15*, 3667−3675.
46. Anzick, S. L., Kononen, J., Walker, R. L., Azorsa, D. O., Tanner, M. M., Guan, X. Y., Sauter, G., Kallioniemi, O. P., Trent, J. M., and Meltzer, P. S. (1997) AIB1, a steroid receptor coactivator amplified in breast and ovarian cancer, *Science 277*, 965−968.
47. Heery, D. M., Hoare, S., Hussain, S., Parker, M. G., and Sheppard, H. (2001) Core LXXLL motif sequences in CREB-binding protein, SRC1, and RIP140 define affinity and selectivity for steroid and retinoid receptors, *J. Biol. Chem. 276*, 6695−6702.
48. Rachez, C., Gamble, M., Chang, C. P., Atkins, G. B., Lazar, M. A., and Freedman, L. P. (2000) The DRIP complex and SRC-1/p160 coactivators share similar nuclear receptor binding determinants but constitute functionally distinct complexes, *Mol. Cell. Biol. 20*, 2718−2726.
49. Cavailles, V., Dauvois, S., L'Horset, F., Lopez, G., Hoare, S., Kushner, P. J., and Parker, M. G. (1995) Nuclear factor RIP140 modulates transcriptional activation by the estrogen receptor, *EMBO J. 14*, 3741−3751.
50. Puigserver, P., Wu, Z., Park, C. W., Graves, R., Wright, M., and Spiegelman, B. M. (1998) A cold-inducible coactivator of nuclear receptors linked to adaptive thermogenesis, *Cell 92*, 829−839.
51. Caira, F., Antonson, P., Pelto-Huikko, M., Treuter, E., and Gustafsson, J. A. (2000) Cloning and characterization of RAP250, a novel nuclear receptor coactivator, *J. Biol. Chem. 275*, 5308−5317.
52. Chang, C., Norris, J. D., Gron, H., Paige, L. A., Hamilton, P. T., Kenan, D. J., Fowlkes, D., and McDonnell, D. P. (1999) Dissection of the LXXLL nuclear receptor-coactivator interaction motif using combinatorial peptide libraries: discovery of peptide antagonists of estrogen receptors alpha and beta, *Mol. Cell. Biol. 19*, 8226−8239.
53. Heldring, N., Nilsson, M., Buehrer, B., Treuter, E., and Gustafsson, J. A. (2004) Identification of tamoxifen-induced coregulator interaction surfaces within the ligand-binding domain of estrogen receptors, *Mol. Cell. Biol. 24*, 3445−3459.
54. Chen, J. D., and Evans, R. M. (1995) A transcriptional co-repressor that interacts with nuclear hormone receptors, *Nature 377*, 454−457.
55. Perissi, V., Staszewski, L. M., McInerney, E. M., Kurokawa, R., Krones, A., Rose, D. W., Lambert, M. H., Milburn, M. V., Glass, C. K., and Rosenfeld, M. G. (1999) Molecular determinants of nuclear receptor-corepressor interaction, *Genes Dev. 13*, 3198−3208.
56. Chang, C. Y., and McDonnell, D. P. (2002) Evaluation of ligand-dependent changes in AR structure using peptide probes, *Mol. Endocrinol. 16*, 647−660.
57. Chang, C. Y., Abdo, J., Hartney, T., and McDonnell, D. P. (2005) Development of peptide antagonists for the androgen receptor using combinatorial peptide phage display, *Mol. Endocrinol. 19*, 2478−2490.
58. Thomas, D. D., Carlsen, W. F., and Stryer, L. (1978) Fluorescence energy transfer in the rapid-diffusion limit, *Proc. Natl. Acad. Sci. U.S.A. 75*, 5746−5750.
59. Zhou, G., Cummings, R., Li, Y., Mitra, S., Wilkinson, H. A., Elbrecht, A., Hermes, J. D., Schaeffer, J. M., Smith, R. G., and Moller, D. E. (1998) Nuclear receptors have distinct affinities for coactivators: characterization by fluorescence resonance energy transfer, *Mol. Endocrinol. 12*, 1594−1604.
60. Wong, C., Kelce, W. R., Sar, M., and Wilson, E. M. (1995) Androgen receptor antagonist versus agonist activities of the fungicide vinclozolin relative to hydroxyflutamide, *J. Biol. Chem. 270*, 19998−20003.
61. Peterziel, H., Culig, Z., Stober, J., Hobisch, A., Radmayr, C., Bartsch, G., Klocker, H., and Cato, A. C. (1995) Mutant androgen receptors in prostatic tumors distinguish between amino-acid-sequence requirements for transactivation and ligand binding, *Int. J. Cancer 63*, 544−550.
62. Lin, M. F., Kawachi, M. H., Stallcup, M. R., Grunberg, S. M., and Lin, F. F. (1995) Growth inhibition of androgen-insensitive human prostate carcinoma cells by a 19-norsteroid derivative agent, mifepristone, *Prostate 26*, 194−204.
63. Cheng, S., Brzostek, S., Lee, S. R., Hollenberg, A. N., and Balk, S. P. (2002) Inhibition of the dihydrotestosterone-activated androgen receptor by nuclear receptor corepressor, *Mol. Endocrinol. 16*, 1492−1501.
64. Gowda, K., Marks, B. D., Zielinski, T. K., and Ozers, M. S. (2006) Development of a coactivator displacement assay for the orphan receptor estrogen-related receptor-gamma using time-resolved fluorescence resonance energy transfer, *Anal. Biochem 357*, 105−115.
65. Selvin, P. R., and Hearst, J. E. (1994) Luminescence energy transfer using a terbium chelate: improvements on fluorescence energy transfer, *Proc. Natl. Acad. Sci. U.S.A. 91*, 10024−10028.
66. Selvin, P. R. (2002) Principles and biophysical applications of lanthanide-based probes, *Annu. Rev. Biophys. Biomol. Struct. 31*, 275−302.

BI061321B